NORGES TEKNISK-NATURVITENSKAPELIGE UNIVERSITET

Marked point model of calcites conditioned to seismic data and well data

by

Alfhild Lien Eide and Anne Randi Syversveen

PREPRINT
STATISTICS NO. 9/1999

NORWEGIAN UNIVERSITY OF SCIENCE AND TECHNOLOGY
TRONDHEIM, NORWAY

This report has URL http://www.math.ntnu.no/preprint/statistics/1999/S9-1999.ps
Alfhild Lien Eide has homepage: http://www.math.ntnu.no/~aeide
E-mail: aeide@@math.ntnu.no
Address: Department of Mathematical Sciences, Norwegian University of Science and Technology, N-7491 Trondheim, Norway.

Marked point model of calcites conditioned to seismic data and well data

Alfhild Lien Eide and Anne Randi Syversveen
Department of Mathematical Sciences
Norwegian University of Science and Technology
Trondheim, Norway
aeide@stat.ntnu.no

Abstract

Seismic data give good spatial coverage of the reservoir, though with low resolution. Since acoustic impedance often can be correlated with porosity and/or facies, acoustic impedance derived from seismic data is frequently used as input to stochastic reservoir models. To capture more of the uncertainty in the seismic inversion, stochastic modeling should also be used when modeling acoustic impedance.

A new stochastic model is developed for calcite cemented objects in a sandstone background. Using this model, it is possible to sample the conditional distribution given seismic amplitude data and well data. The background sandstone is modeled with a variable, but low impedance. The calcite objects have a high impedance compared with the background. Seismic forward modeling shows that both the background and the calcites contribute to the seismic response. The model presented is a superposition of a marked point model for the calcites and a continuous model for the background. The presentation is illustrated with a synthetic test case.

1 Introduction

Description of reservoir heterogeneities is important for predicting production from hydrocarbon reservoirs. Calcite cemented sandstones may act as flow barriers in hydrocarbon reservoirs. These calcite cemented layers may occur as small nodules and field-wide barriers, see Bjørkum & Walderhaug (1990).

Stochastic modeling provides a framework for integration of different sources of information about the reservoir, both a priori geology knowledge and reservoir specific information. In this paper we consider two types of reservoir specific information: well data and seismic data.

Increased quality of seismic data makes it feasible to use seismic data not only for structural characterization, but also for characterization of reservoir heterogeneities. Seismic data give almost exhaustive spatial coverage, but since the relation between seismic data and reservoir properties is indirect, this calls for stochastic models that can handle this indirect relation. Doyen (1988) uses cokriging to estimate the areal distribution of porosity. Zhu & Journel (1993) use indicator kriging where seismic data are used to provide local probability distributions. Tjølsen et al. (1995) and Skare et al. (1997) use seismic impedance to guide the location of fluvial sandstone bodies in a stochastic reservoir model. Behrens, MacLeod & Tran (1996) and Doyen et al. (1997) use block kriging to correct for the different volumes of support for seismic data and well data.

In the previously mentioned models it is assumed that acoustic impedance is available from conventional inversion methods. Bortoli et al. (1993) and Haas & Dubrule (1994) suggest using stochastic models at an earlier stage in the inversion process. Stochastic modeling is used to generate high-resolution images of acoustic impedance conditioned to seismic amplitude. The model incorporates a physical seismic forward model, convolution with a seismic wavelet, in the likelihood linking seismic data to the acoustic impedances. Due to the nonlinear relation between seismic amplitude and acoustic impedance, iterative sampling techniques are used. Abrahamsen et al. (1997) use a more formal approach and improve the efficiency of the sampling by utilizing a linearized model. Eide, Ursin & Omre (1997) avoid the iterative sampling and matching problem by using the linear relation between seismic amplitude and reflection coefficients under the convolution model. The reflection coefficients are modeled as a Gaussian random field. Under these assumptions the posterior distribution of reflection coefficients conditioned to reflection coefficient well data and seismic amplitude data can be obtained analytically. A nonlinear, deterministic transformation takes realizations of reflection coefficients into realizations of acoustic impedance which is used for modeling porosity.

In this paper, the model from Eide et al. (1997) is combined with a marked point model for calcite cemented objects. The use of marked point models for facies units goes back to Haldorsen & Lake (1984). Later on, these models have been refined and developed in a variety of ways. Syversveen & Omre (1997) present a marked point model for facies objects conditioned to well data. Their model can handle conditioning on observations from more than one well for each object. In the current paper, the model is merged with the model from Eide et al. (1997) to handle conditioning to seismic amplitude data. Furthermore, the model is combined with a Gaussian based model for the background facies, see Eide et al. (1997).

1.1 Overview of model

The model is developed in a Bayesian framework where general geoscience knowledge and experience from similar reservoirs can be included in the prior probability density function (pdf), while reservoir specific observations such as well data and seismic data are included using their respective forward models to define the likelihood functions. The objective is to sample the posterior pdf

$$f(\boldsymbol{z}, \boldsymbol{l} | \boldsymbol{z}^o, \boldsymbol{l}^o, \boldsymbol{s}^o) \tag{1}$$

of acoustic impedance $\boldsymbol{Z}$ and facies $\boldsymbol{L}$ in the reservoir given acoustic impedance well data $\boldsymbol{z}^o$, facies well data $\boldsymbol{l}^o$ and seismic data $\boldsymbol{s}^o$.

In Section 2 the prior model of the reservoir is defined. This model is a combination of a Gaussian random field and a marked point model.

In Section 3, the likelihood functions linking reservoir specific observations to the reservoir variables are discussed. Two types of reservoir specific observations are considered: well data and seismic data. Well data have a high vertical resolution but are spatially sparse. Seismic data have a lower resolution but are spatially dense. Seismic data measure changes in acoustic impedance. The reflected amplitude due to a change in impedance is proportional to the relative change in impedance; when impedance changes from $Z(x_i, t_j)$ to $Z(x_i, t_{j+1})$ the reflection coefficient is

$$C(x_i, t_i) = \frac{Z(x_i, t_{j+1}) - Z(x_i, t_j)}{Z(x_i, t_{j+1}) + Z(x_i, t_j)}. \tag{2}$$

Reflection coefficients are linearly related to seismic amplitude under a convolution model. The convolution model is linear and fast, hence easy to combine with the iterative sampling techniques required for sampling the posterior pdf of the calcite objects. In an appendix to this paper, seismic response from a series of thin calcites using a convolution model is compared with seismic response using a full waveform reflectivity model. The convolution model is simpler, but is found to give acceptable results.

In Section 4, the posterior pdf of facies and acoustic impedance given seismic data and well data is given. With the model described, the posterior distribution can be sampled sequentially. This is discussed in Section 5. A simulation example is given in Section 6.

2 A priori reservoir model

The following reservoir model consisting of two facies types is assumed: The background facies is a sandstone with a variable but relatively low impedance. The foreground is calcite cemented objects with a higher impedance. The high impedance of the calcites typically give high reflection coefficients at the interfaces between sandstone and calcite. The reflection coefficient at the interface between sandstone and calcite will be denoted c_p.

The model is described for a 2D vertical cross section through the reservoir, although the idea can also be extended to 3D.

2.1 Calcites

The calcites are modeled by a marked point model similar to the model used by Syversveen & Omre (1997) for modeling shales in a sandstone reservoir. Each calcite is modeled as a rectangle superimposed by a deformation at the top and bottom, see Figure 1.

The parameter vector $\mathbf{\Theta}$ contains center-point (X_i, T_i), length B_i and height H_i of each rectangle. The random functions $\boldsymbol{Y}_i(\cdot) = [\boldsymbol{Y}_{iT}(\cdot)\ ,\ \boldsymbol{Y}_{iB}(\cdot)]$ represent the deformations at the top and the bottom. The expected height of the calcite is the height of the rectangle, while the length of the calcite equals the length of the rectangle. The number of calcites N is also stochastic. In the prior distribution it is assumed that the horizontal and vertical dimensions of each calcite are independent.

The deformations at the top and the bottom provide a flexible model that can handle conditioning to well data where the same object is observed in several wells, see Syversveen & Omre (1997).

The joint density for the N calcites can be written

$$f(\boldsymbol{\theta}, n, \boldsymbol{y}(\cdot)) = f(\boldsymbol{\theta}, n) f(\boldsymbol{y}(\cdot)|\boldsymbol{\theta}, n). \tag{3}$$

The prior pdf of $\mathbf{\Theta}$ and N is defined by a marked point model, see Stoyan, Kendall & Mecke (1987), with pairwise interaction of the form

$$f(\boldsymbol{\theta}, n) = \text{const} \cdot \exp\{\sum_{i=1}^{n}(\beta_1(x_i, b_i) + \beta_2(t_i, h_i)) + \sum_{j=1}^{n}\sum_{i<j} d((x_i, t_i), (x_j, t_j)) + na\}. \tag{4}$$

The first term of the exponent, $(\beta_1(x_i, b_i) + \beta_2(t_i, h_i))$ represents the marginal characteristics of the calcites, while the next term $d((x_i, t_i), (x_j, t_j))$ is a pairwise interaction function between center-points of calcites, and the last term is related to the intensity of calcites. In order to obtain the parts of the posterior pdf related to the vertical parameters T_i and H_i analytically, the function $\exp(\beta_2(t_i, h_i))$ is defined to be a truncated bi-Gaussian pdf. The variance of T_i is usually chosen large, to approximate a uniform distribution over the domain. The function $\exp(\beta_1(x_i, b_i))$ can be chosen to be any suitable pdf according to geological experience. We let X_i have a uniform distribution over the domain, and B_i have a Gaussian distribution. See Syversveen & Omre (1997) for a complete explanation.

The deformations $\boldsymbol{Y}_i$ are modeled as Gaussian random fields. We assume that the stochastic fields $[\boldsymbol{Y}_i|\boldsymbol{\Theta}_i = \boldsymbol{\theta}_i]$ in different calcites are conditionally independent, which gives

$$f(\boldsymbol{y}(\cdot)|\boldsymbol{\theta}, n) = \prod_{i=1}^{n} f(\boldsymbol{y}(\cdot)|\boldsymbol{\theta}_i). \tag{5}$$

2.2 Sandstone background facies

The background facies has a variable, but low acoustic impedance. For computational reasons, the stochastic model for the variations in the background is defined by the reflection coefficients. There is a deterministic, nonlinear relation between reflection coefficients and acoustic impedance.

The reflection coefficients in the sandstone background are modeled as a Gaussian random field discretized on a grid. The vector $\boldsymbol{C}$ contains the reflection coefficients on the grid, with

$$\mathrm{E}[\boldsymbol{C}] = \boldsymbol{\mu}_C, \tag{6}$$
$$\mathrm{Cov}[\boldsymbol{C}] = \Sigma_C, \tag{7}$$

where $\boldsymbol{\mu}_C$ is the expected level of the reflection coefficients. The covariance matrix Σ_C is defined by the variance σ_C and the spatial correlation function $\rho_C(\cdot,\cdot)$ of the reflection coefficients. It is assumed that the distribution of reflection coefficients in the background sandstone is independent of the positions of the calcites.

3 Likelihood model

Two types of data are available: Well data and seismic data. These are assumed to be conditionally independent given the reservoir. Seismic data are usually given with seismic travel time as depth reference. Here it will be assumed that the well data have been converted from depth to time, hence that both seismic data and well data have the same vertical reference t.

3.1 Seismic data

Seismic data $\boldsymbol{S}^o$ are modeled with a convolution between reflection coefficients and a seismic pulse or wavelet. This is a linear model where the seismic response can be written as a sum of two parts, one from the Gaussian background and another from the calcites described by $\boldsymbol{\theta}$. In addition we assume an error term $\boldsymbol{U}_S$.

$$[\boldsymbol{S}^o|\boldsymbol{C}=\boldsymbol{c},\boldsymbol{\Theta}=\boldsymbol{\theta},N=n] = A_s\boldsymbol{c}+\boldsymbol{g}_s(\boldsymbol{\theta},n)+\boldsymbol{U}_S \tag{8}$$

where A_s is a matrix defined by the seismic wavelet, such that $A_s\boldsymbol{c}$ is the seismic response from the background and $\boldsymbol{g}_s(\boldsymbol{\theta},n)$ is the seismic response from the n calcites with location and size given by $\boldsymbol{\theta}$.

Assume that $\boldsymbol{U}_S$ is Gaussian with mean zero and covariance matrix Σ_S. Then the conditional distribution of $\boldsymbol{S}^o$ given $(\boldsymbol{\Theta},N)$, is Gaussian with

$$\mathrm{E}[\boldsymbol{S}^o|\boldsymbol{\Theta}=\boldsymbol{\theta},N=n] = \boldsymbol{m}_{S^o|\Theta,N} = A_s\boldsymbol{\mu}_C+\boldsymbol{g}_s(\boldsymbol{\theta},n) \tag{9}$$

$$\mathrm{Cov}[\boldsymbol{S}^o|\boldsymbol{\Theta}=\boldsymbol{\theta},N=n] = \Sigma_{S^o|\Theta,N} = A_s\Sigma_C A_s^T+\Sigma_S \tag{10}$$

The seismic response function for a calcite centered at (x_i,t_i) with length b_i and thickness h_i is assumed to consist of a reflection from the top and a reflection from the bottom. The reflection coefficient c_p at the interface between background and calcite is assumed to be the same for all calcites, regardless of the impedance of the background. This approximation is done for computational reasons, and it can be justified when the impedance difference between sandstone and calcite is large compared with the variability of the sandstone impedance. Furthermore, the seismic response function is assumed to be the same for undeformed and deformed calcites, hence seismic response is independent of $\boldsymbol{y}_{iB}(\cdot)$ and $\boldsymbol{y}_{iT}(\cdot)$. The seismic response in location (x,t) from a set of n calcites in locations (x_i,t_i) with lengths b_i and thicknesses h_i, $i=1\ldots n$ becomes

$$g_s(x,t;\boldsymbol{\theta},n) = \sum_{i=1}^{n} I[x_i-b_i/2<x<x_i+b_i/2]\cdot\{c_p\cdot h[t-(t_i-h_i/2)]-c_p\cdot h[t-(t_i+h_i/2)]\} \tag{11}$$

where I is an indicator function taking the value one whenever the condition in the brackets is fulfilled and zero otherwise, and $h(t)$ is the seismic wavelet.

This is a simplified expression that only accounts for primary reflections. Bakke (1996) has shown that primary reflections account for a relatively large part of the seismic reflections from a thin layer. In an appendix to this paper the convolution model is compared with a full waveform reflectivity model. There is a high correlation between synthetic seismic traces generated by applying the two different forward models to well data from a calcite-cemented sandstone reservoir. The modeling error made by these simplifications is included in the error term $\boldsymbol{U}_S$.

3.2 Well data

The well data are assumed to contain exact observations of the intersection of calcites along the transects of n_w vertical wells. It is also assumed that it is known whether observations from different wells pertain to the same calcite. Furthermore, it is assumed that the well data contain exact observations of acoustic impedance in the background sandstone on the grid nodes intersected by the well.

Observations of the top and bottom of the calcites are contained in the vector $\boldsymbol{l}^o$. Following Syversveen & Omre (1997), the likelihood function for $(\boldsymbol{\Theta}, N)$ can be written

$$f(\boldsymbol{l}^o|\boldsymbol{\Theta}, n) = \text{const} \cdot \prod_{i=1}^{v} f(\boldsymbol{l}_i^o|t_i, h_i) \prod_{j=1}^{n} I(\boldsymbol{l}_j^o|x_j, b_j) \tag{12}$$

where v is the number of calcites penetrated by wells, $f(\boldsymbol{l}_i^o|t_i, h_i)$ is the likelihood model related to depth observations of calcite no i, and $I(\boldsymbol{l}_j^o|x_j, b_j)$ is an indicator function taking the value one whenever the conditioning in the horizontal direction is fulfilled, and zero otherwise. The likelihood model related to depth observations, $f(\boldsymbol{l}_i^o|t_i, h_i)$, is Gaussian since the deformations $\boldsymbol{Y}_i(\cdot)$ are Gaussian.

Well data from the background are assumed to be exact observations of the reflection coefficients at the grid nodes intersected by wells. This model of the well data can be written

$$\boldsymbol{C}^o = A_w \boldsymbol{C} \tag{13}$$

where C^o denotes background reflection coefficients in the wells, calculated from the impedance well data.

Let $\boldsymbol{D}^{(B)} = [\boldsymbol{S}^o, \boldsymbol{C}^o]^T$ denote all observations pertaining to the background. Then

$$[\boldsymbol{D}^{(B)}|\boldsymbol{\theta}, n] = \begin{bmatrix} \boldsymbol{S}^o \\ \boldsymbol{C}^o \end{bmatrix} = \begin{bmatrix} A_s \\ A_w \end{bmatrix} \boldsymbol{C} + \begin{bmatrix} \boldsymbol{g}_s(\boldsymbol{\theta}, n) \\ 0 \end{bmatrix} + \begin{bmatrix} \boldsymbol{U}_S \\ 0 \end{bmatrix} \tag{14}$$

In a compact form,

$$\boldsymbol{D}^{(B)} = A\boldsymbol{C} + \boldsymbol{g}(\boldsymbol{\theta}, n) + \boldsymbol{U}^{(B)} \tag{15}$$

where A, $\boldsymbol{g}(\boldsymbol{\theta}, n)$ and $\boldsymbol{U}^{(B)}$ are defined by Expression (14).

The conditional distribution of $\boldsymbol{D}^{(B)}$ given $(\boldsymbol{\theta}, n)$ is Gaussian with

$$\mathrm{E}[\boldsymbol{D}^{(B)}|\boldsymbol{\Theta} = \boldsymbol{\theta}, N = n] = \boldsymbol{m}_{D^{(B)}|\Theta,N} = A\boldsymbol{\mu}_C + \boldsymbol{g}(\boldsymbol{\theta}, n), \tag{16}$$

$$\mathrm{Cov}[\boldsymbol{D}^{(B)}|\boldsymbol{\Theta} = \boldsymbol{\theta}, N = n] = \Sigma_{D^{(B)}|\Theta,N} = A\Sigma_C A^T + \Sigma^{(B)}. \tag{17}$$

Here $\Sigma^{(B)}$ denotes the covariance matrix of $\boldsymbol{U}^{(B)}$.

4 The posterior distribution

The posterior distribution of background reflection coefficients $\boldsymbol{C}$ and calcites described by $\boldsymbol{L} = (\boldsymbol{\Theta}, N, \boldsymbol{Y})$, given seismic data $\boldsymbol{S}^o$, background reflection coefficients data $\boldsymbol{C}^o$ and calcite well data $\boldsymbol{L}^o$ can be written

$$f(\boldsymbol{c}, \boldsymbol{\theta}, n, \boldsymbol{y} | \boldsymbol{s}^o, \boldsymbol{c}^o, \boldsymbol{l}^o) = f(\boldsymbol{c} | \boldsymbol{\theta}, n, \boldsymbol{y}, \boldsymbol{s}^o, \boldsymbol{c}^o, \boldsymbol{l}^o) \cdot f(\boldsymbol{\theta}, n, \boldsymbol{y} | \boldsymbol{s}^o, \boldsymbol{c}^o, \boldsymbol{l}^o). \tag{18}$$

Assuming the background $\boldsymbol{C}$ to be independent of $\boldsymbol{Y}$ and $\boldsymbol{L}^o$, the term $f(\boldsymbol{c} | \boldsymbol{\theta}, n, \boldsymbol{y}, \boldsymbol{s}^o, \boldsymbol{c}^o, \boldsymbol{l}^o)$ can be replaced by $f(\boldsymbol{c} | \boldsymbol{\theta}, n, \boldsymbol{s}^o, \boldsymbol{c}^o)$. The last factor in Equation (18) can be written

$$\begin{aligned} f(\boldsymbol{\theta}, n, \boldsymbol{y} | \boldsymbol{s}^o, \boldsymbol{c}^o, \boldsymbol{l}^o) &= f(\boldsymbol{y} | \boldsymbol{\theta}, n, \boldsymbol{s}^o, \boldsymbol{c}^o, \boldsymbol{l}^o) f(\boldsymbol{\theta}, n | \boldsymbol{s}^o, \boldsymbol{c}^o, \boldsymbol{l}^o) \\ &= f(\boldsymbol{y} | \boldsymbol{\theta}, n, \boldsymbol{l}^o) f(\boldsymbol{\theta}, n | \boldsymbol{s}^o, \boldsymbol{c}^o, \boldsymbol{l}^o), \end{aligned} \tag{19}$$

where the first term on the right hand side was simplified because $\boldsymbol{Y}$ is independent of $\boldsymbol{S}^o$ and $\boldsymbol{C}^o$. The last term of Equation (19), which is the posterior distribution of $(\boldsymbol{\Theta}, N)$ given the data $(\boldsymbol{S}^o, \boldsymbol{C}^o, \boldsymbol{L}^o)$, can be written

$$\begin{aligned} f(\boldsymbol{\theta}, n | \boldsymbol{s}^o, \boldsymbol{c}^o, \boldsymbol{l}^o) &= \text{const} \cdot f(\boldsymbol{s}^o, \boldsymbol{c}^o, \boldsymbol{l}^o | \boldsymbol{\theta}, n) f(\boldsymbol{\theta}, n) \\ &= \text{const} \cdot f(\boldsymbol{s}^o, \boldsymbol{l}^o | \boldsymbol{c}^o, \boldsymbol{\theta}, n) f(\boldsymbol{c}^o | \boldsymbol{\theta}, n) f(\boldsymbol{\theta}, n) \\ &= \text{const} \cdot f(\boldsymbol{s}^o | \boldsymbol{c}^o, \boldsymbol{\theta}, n) f(\boldsymbol{l}^o | \boldsymbol{c}^o, \boldsymbol{\theta}, n) f(\boldsymbol{c}^o) f(\boldsymbol{\theta}, n) \\ &= \text{const} \cdot f(\boldsymbol{s}^o | \boldsymbol{c}^o, \boldsymbol{\theta}, n) f(\boldsymbol{l}^o | \boldsymbol{\theta}, n) f(\boldsymbol{\theta}, n). \end{aligned} \tag{20}$$

Combining this with Equations (18) and (19), we have

$$\begin{aligned} f(\boldsymbol{c}, \boldsymbol{\theta}, n, \boldsymbol{y} | \boldsymbol{s}^o, \boldsymbol{c}^o, \boldsymbol{l}^o) = \text{const} &\cdot f(\boldsymbol{c} | \boldsymbol{\theta}, n, \boldsymbol{s}^o, \boldsymbol{c}^o) \cdot f(\boldsymbol{y} | \boldsymbol{\theta}, n, \boldsymbol{l}^o) \\ &\cdot f(\boldsymbol{s}^o | \boldsymbol{c}^o, \boldsymbol{\theta}, n) \cdot f(\boldsymbol{l}^o | \boldsymbol{\theta}, n) \cdot f(\boldsymbol{\theta}, n). \end{aligned} \tag{21}$$

To be able to sample the posterior pdf given in Equation (21), the likelihood function $f(\boldsymbol{s}^o | \boldsymbol{c}^o, \boldsymbol{\theta}, n)$ for observing seismic data $\boldsymbol{s}^o$ given background reflection coefficients well data $\boldsymbol{c}^o$ and calcite configuration $(\boldsymbol{\theta}, n)$ is needed.

The conditional distribution of $\boldsymbol{S}^o$ given $(\boldsymbol{\Theta}, N)$ is Gaussian with mean given by Equation (9) and covariance matrix given by Equation (10). Similarly the conditional distribution of $\boldsymbol{C}^o$ given $(\boldsymbol{\Theta}, N)$ is Gaussian with mean $A_w \boldsymbol{\mu}_c$ and covariance matrix $A_w \Sigma_C A_w^T$. Combining this gives

$$\begin{aligned} \mathrm{E}[\boldsymbol{S}^o | \boldsymbol{C}^o = \boldsymbol{c}^o, \boldsymbol{\Theta} = \boldsymbol{\theta}, N = n] &= \boldsymbol{m}_{S^o | C^o, \Theta, N} \\ &= \boldsymbol{m}_{S^o | \Theta, N} + A_s \Sigma_C A_w^T (A_w \Sigma_C A_w^T)^{-1} (\boldsymbol{c}^o - A_w \boldsymbol{\mu}_c) \end{aligned} \tag{22}$$

$$\begin{aligned} \mathrm{Cov}[\boldsymbol{S}^o | \boldsymbol{C}^o = \boldsymbol{c}^o, \boldsymbol{\Theta} = \boldsymbol{\theta}, N = n] &= \Sigma_{S^o | C^o, \Theta, N} \\ &= \Sigma_{S^o | \Theta, N} - A_s \Sigma_C A_w^T (A_w \Sigma_C A_w^T)^{-1} A_w \Sigma_C A_s^T. \end{aligned} \tag{23}$$

This model gives the following likelihood function:

$$f(\boldsymbol{s}^o|\boldsymbol{c}^o,\boldsymbol{\theta},n) = \text{const}\cdot|\Sigma_{S^o|C^o,\Theta,N}|^{-1/2}\exp\{-\frac{1}{2}(\boldsymbol{s}^o-\boldsymbol{m}_{S^o|C^o,\Theta,N})^T\Sigma^{-1}_{S^o|C^o,\Theta,N}(\boldsymbol{s}^o-\boldsymbol{m}_{S^o|C^o,\Theta,N})\}.$$

The covariance matrix $\Sigma_{S^o|C^o,\Theta,N}$ is not a function of $(\boldsymbol{C}^o,\boldsymbol{\Theta},N)$ and hence $|\Sigma_{S^o|C^o,\Theta,N}|^{-1/2}$ can be taken as part of the constant:

$$f(\boldsymbol{s}^o|\boldsymbol{c}^o,\boldsymbol{\theta},n) = \text{const}\cdot\exp\{-\frac{1}{2}(\boldsymbol{s}^o-\boldsymbol{m}_{S^o|C^o,\Theta,N})^T\Sigma^{-1}_{S^o|C^o,\Theta,N}(\boldsymbol{s}^o-\boldsymbol{m}_{S^o|C^o,\Theta,N})\}. \quad (24)$$

5 Simulation algorithm

The first term on the right hand side in the posterior distribution, see Equation (21), is Gaussian with mean and standard deviation given by

$$\begin{aligned}
&\mathrm{E}[\boldsymbol{C}|\boldsymbol{\Theta}=\boldsymbol{\theta},N=n,\boldsymbol{D}^{(B)}=\boldsymbol{d}^{(B)}] = \\
&\qquad \boldsymbol{\mu}_C + \Sigma_C A^T(\Sigma_{D^{(B)}|\Theta,N})^{-1}(\boldsymbol{d}^{(B)}-\boldsymbol{m}_{D^{(B)}|\Theta,N}) \qquad (25)\\
&\mathrm{Cov}[\boldsymbol{C}|\boldsymbol{\Theta}=\boldsymbol{\theta},N=n,\boldsymbol{D}^{(B)}=\boldsymbol{d}^{(B)}] = \\
&\qquad \Sigma_C - \Sigma_C A^T(\Sigma_{D^{(B)}|\Theta,N})^{-1}A\Sigma_C \qquad (26)
\end{aligned}$$

The second term is also Gaussian, see Syversveen & Omre (1997), and can be sampled directly, while the remaining terms must be sampled using Markov chain Monte Carlo methods.

Syversveen & Omre (1997) sample facies objects conditioned to well data by sampling a pdf proportional to $f(\boldsymbol{l}^o|\boldsymbol{\theta},n)\cdot f(\boldsymbol{\theta},n)$ using the Metropolis-Hastings algorithm (Hastings 1970). The algorithm used by Syversveen & Omre (1997) can easily be modified to sample calcite objects conditioned to seismic data and well data by sampling a pdf proportional to $f(\boldsymbol{s}^o|\boldsymbol{c}^o,\boldsymbol{\theta},n)\cdot f(\boldsymbol{l}^o|\boldsymbol{\theta},n)\cdot f(\boldsymbol{\theta},n)$. This amounts to multiplying the acceptance probability with the fraction $f(\boldsymbol{s}^o|\boldsymbol{c}^o,\boldsymbol{\theta}',n')/f(\boldsymbol{s}^o|\boldsymbol{c}^o,\boldsymbol{\theta},n)$ where $(\boldsymbol{\theta},n)$ and $(\boldsymbol{\theta}',n')$ are the old and the potential new calcite configurations respectively and $f(\boldsymbol{s}^o|\boldsymbol{c}^o,\boldsymbol{\theta},n)$ is the seismic likelihood given in Equation (24).

Again following Syversveen & Omre (1997), the transition proposal kernel used in the Metropolis-Hastings algorithm for this problem consists of three types of transitions: With probability $1-2\beta$ alter one calcite randomly chosen among all calcites observed in wells, with probability β add a new calcite not intersecting any well, and with probability β delete a calcite randomly chosen among all calcites not intersecting any wells. Due to the conditioning, it is impossible to add or delete a calcite observed in the wells.

This gives the following procedure for sampling the posterior probability given in Equation (21):

1. Simulate undeformed calcite objects conditioned to seismic data and well data by sampling $f(\boldsymbol{\theta}, n|\boldsymbol{s}^o, \boldsymbol{c}^o, \boldsymbol{l}^o) = \text{const}\cdot f(\boldsymbol{s}^o|\boldsymbol{c}^o, \boldsymbol{\theta}, n)\cdot f(\boldsymbol{l}^o|\boldsymbol{\theta}, n)\cdot f(\boldsymbol{\theta}, n)$ using the Metropolis-Hastings algorithm.

2. Simulate the deformations conditioned to well observations by sampling $f(\boldsymbol{y}|\boldsymbol{\theta}, n, \boldsymbol{l}^o)$. This is a 1D Gaussian random function, see Syversveen & Omre (1997).

3. Simulate the background reflection coefficients conditioned to calcite objects, seismic data and well data. That is, sample $f(\boldsymbol{c}|\boldsymbol{\theta}, n, \boldsymbol{s}^o, \boldsymbol{c}^o)$ by simulating a 2D Gaussian random function with mean and covariance as given in Equations (25) and (26).

As mentioned in Section 3.1, the observed seismic response is modeled as a sum of the seismic response from the background and the seismic response from the calcites. However, we have now shown that with a Gaussian assumption on the background reflection coefficients, it is possible to sample the calcites separately before sampling the background. In Equation (10) and (23) above, the effect of the reflection coefficients in the background is a term that can be viewed as a noise term when sampling the calcites. Note however that the well observations of the background reflection coefficients influence the likelihood of the seismic data near the wells, see Equation (24), due to the spatial model on the reflection coefficients. The covariance matrix $\Sigma_{S^o|C^o,\Theta,N}$ in the likelihood, see Equation (24), is not a function of $\boldsymbol{\theta}$ and only needs to be computed once. If the dimension of $\boldsymbol{S}^o$ is large, some approximations may be needed to simplify the expression.

Finally, the field of reflection coefficients $C(x_i, t_j)$ simulated in step 3 above can be converted to impedance $Z(x_i, t_j)$ using the relation

$$Z(x_i, t_{j+1}) = \frac{1 + C(x_i, t_j)}{1 - C(x_i, t_j)} Z(x_i, t_j) \tag{27}$$

and set of starting values $Z(x_i, t_0)$.

6 Simulation example

A simple simulation example is performed on a 2D vertical cross section. The reservoir thickness corresponds to 25 ms travel time. The width corresponds to 25 seismic traces. There are two vertical wells penetrating the reservoir.

The background is discretized on a 25×25 grid. Each grid node is 2×2 units. The vertical size of each grid cell is 1 ms. The wells are located at $x = 30$ and $x = 49$.

The prior model for the calcites is a marked point model as defined in section 2.1. For each calcite the depth coordinate T_i and the height H_i are assumed independent. The distribution of T_i of the center points is a truncated Gaussian distribution with mean $\mu_T = 25$ and variance $\sigma_T^2 = 75^2$. The expected thickness of calcites is $\mu_H = 1$ with a variance of $\sigma_H^2 = 0.4$. The expected length is $\mu_L = 22.0$ with a variance of $\sigma_L^2 = 15^2$. The horizontal center points X_i are assumed to be uniformly distributed on the domain. The intensity parameter a is set to 3. The spatial interaction is defined to be

$$d((x_i,t_i),(x_j,t_j)) = \begin{cases} \ln\left(\frac{\|(x_i,t_i)-(x_j,t_j)\|}{30}\right) & \text{if } \|(x_i,t_i)-(x_j,t_j)\| \le 30, \\ 0 & \text{otherwise.} \end{cases} \tag{28}$$

The deformations at the top and the bottom are Gaussian random fields with mean zero and variance 0.48. The covariance between the top and the bottom is 0.2. The correlation function of each surface is defined to be $\rho_Y(x) = \exp(-0.05|x|)$.

The reflection coefficient between background sandstone and calcite, c_p is set to 0.3.

The background reflection coefficients are described as a Gaussian random field with mean $\mu_C = 0$, variance 0.03^2 and correlation function being a standardized version of the covariance function of a difference, see Eide (1998).

$$\begin{aligned} \mathrm{Cov}(C_{i,j}, C_{k,l}) &\approx \frac{1}{4\mathrm{E}[Z]^2}\mathrm{Cov}(Z_{i,j+1} - Z_{i,j}, Z_{k,l+1} - Z_{k,l}) \\ &= \frac{\sigma_Z^2}{4\mathrm{E}[Z]^2}[2\rho(Z_{i,j}, Z_{k,l}) - \rho(Z_{i,j+1}, Z_{k,l}) - \rho(Z_{i,j}, Z_{k,l+1})] \end{aligned} \tag{29}$$

where $\rho(Z_{i,j}, Z_{k,l}) = \exp\{-3[(i-k)^2/a_x^2 + (j-l)^2/a_t^2]^\nu\}$ with $a_x = 30$, $a_t = 2$ and $v = 1.2$. The indices i, j, k, l refer to grid nodes.

A realization from the prior model is taken to be the true reservoir, see Figure 2. From this, well data from the two wells and seismic data from 25 seismic traces are generated. The seismic data are shown in Figure 3.

In the posterior distribution, the parameters μ_H and σ_H^2 are estimated by empirical Bayes. The intensity parameter a and interaction parameters may also be estimated, see Syversveen & Rue (1997). In this example however, we assume that these parameters are known. The rest of the parameters are also assumed known in the posterior.

In the Metropolis-Hastings algorithm the parameter β is set to 0.2 and 150 000 iterations are performed. Figure 4 shows the number of calcites and the seismic log-likelihood plotted vs the number of iterations. The plot indicates that the number of calcites and the seismic likelihood function have stabilized before 150 000 iterations, which indicates that this number of iterations is sufficient for convergence of the algorithm.

Figure 5 shows four realizations from the posterior distribution. The calcite well observations have been reproduced. Some of the calcite objects not observed in the wells are also reproduced, but here there is more variability. The extension of the two uppermost calcites is reproduced in most realizations. These calcites are observed in the wells, but the extension is controlled by the seismic data. In some realizations, the long, thin calcite on the lower left hand side in the cross section of the true reservoir has been replaced by an elongation of the calcite just above, which is observed in a well. Note also the calcite in the lower right corner of the true cross section. This one is not observed in any wells, but all the realizations shown here have a calcite object near this location. The synthetic seismic shown in Figure 6 shows that the seismic data are reproduced by all the realizations.

7 Conclusion

We have presented a stochastic model for calcite cemented facies objects in a sandstone background. The model can be conditioned to well data and seismic data. This model merges a continuous model for the impedance in the sandstone background with a marked point model for the calcite cemented objects. To simplify the posterior distribution, it is assumed that the reflection coefficients in the background can be described by a Gaussian random field.

The seismic forward model can be split into two parts. The first part is a linear relation between seismic data and the reflection coefficients in the background sandstone. The second part is a nonlinear relation between the seismic data and the marked point model of the calcites.

The posterior distribution of facies objects and background can be sampled sequentially by first sampling the facies objects using Metropolis-Hastings algorithm, then sampling the background reflection coefficients. The posterior distribution of reflection coefficients conditioned on seismic data, well data and the location and size of facies objects can be obtained analytically.

The simulated realizations of acoustic impedance can be used together with porosity well data for stochastic simulation of porosity, see Eide et al. (1997).

Appendix: Comparison of seismic forward models for stochastic modeling of calcites

In this appendix two different seismic forward models for use in stochastic modeling of thin calcite barriers in a sandstone background are compared. The comparison is done using real well data from the Troll field in the North Sea.

A full waveform reflectivity (f-k) model will be compared with a convolution model with a Ricker wavelet. The full waveform reflectivity model gives an exact solution to the wave equation for horizontally stratified media, see Kennett (1983). The convolution model only includes primary reflections, that is, no multiples or converted waves. According to Appendix A of Bakke (1996), the primaries account for a relatively large part of the seismic signal from a thin layer. The convolution model for the seismic response is linear and fast, hence easy to combine with the iterative sampling techniques frequently needed in stochastic reservoir modeling.

The well data used here are blocked acoustic impedance logs from two wells in the TOGI (Troll Oseberg Gas Injection) part of the Troll Field in the North Sea. These data have previously been studied by Bakke et al. (1996). The reservoir zone studied consists of a set of thin calcite barriers in a sandstone background. The acoustic impedance of the sandstone varies around $0.4 \cdot 10^7 - 0.5 \cdot 10^7$ kg/m^3 m/s. The most important reservoir heterogeneities are the calcite barriers. These calcite barriers have a high impedance ($1.7 \cdot 10^7$ kg/m^3 m/s) compared with the sandstone background. Bakke et al. (1996) have shown that the concentration of thin calcite beds around bounding surfaces produces a measurable seismic response in this reservoir model.

To compare the results from the simplified convolution model and the full waveform reflectivity model, the seismic responses from the two models have been examined using the impedance data at the two wells. Figure 7 shows the impedance log in the first well, reflection coefficients calculated from the impedances, and the seismic response obtained by convolution of the reflection coefficients with a 40 Hz Ricker wavelet. This is compared with the seismic response from the full waveform reflectivity model. Figure 8 shows a similar plot for the second well. The correlation between the seismic response calculated by convolution and the corresponding trace from the full waveform reflectivity model is 0.87 for the first well and 0.79 for the second. These large correlations are in accordance with the results from Bakke (1996), where it is shown that the primaries account for a relatively large part of the seismic reflections from a thin layer.

The seismic response from the background and the calcite barriers in the convolution model can formally be written

$$(S|R = r, \Psi = \psi) = h(\psi_1) * r_b + h(\psi_2) * r_c + U \tag{30}$$

where S denotes seismic observations, $r = (r_b, r_c)$ denotes the reflection coefficients from background and calcite barriers respectively, $h(\cdot)$ is the seismic pulse, $\psi = (\psi_1, \psi_2)$ are pulse shape parameters and U is random noise.

To see how much the background contributes to the seismic response under the convolution model, the impedances and reflection coefficients have been split as shown in Figures 9 and 10. The corresponding seismic responses calculated by the convolution model with $\psi_1 = \psi_2 = 40$ are shown in 11. These figures show that removal of the calcite barriers reduces the correlations with the corresponding traces from the full waveform model, where calcite barriers are still included, from 0.871 to 0.697 for the first well and from 0.793 to 0.591 for the second well.

Whenever a simplified seismic forward model is used, a modeling error is introduced. The large correlations of about 0.8 in Figures 7 and 8 indicate that this error is not too large in this case. The error also depends on the pulse parameters ψ_1 and ψ_2. To check whether other values of ψ_1 and ψ_2 give even higher correlations between the results from the convolution model and the full waveform model, correlations have been calculated on a grid of (ψ_1, ψ_2) values centered around 40 Hz. The results are shown in Figures 12 and 13. These figures show that the optimal values of ψ_1 and ψ_2 in those two wells are not 40 Hz as used in the full waveform reflectivity model. For well 1, the optimal correlation of 0.873 is obtained at $\psi_1 = 41.6$ and $\psi_2 = 39.7$. For well 2, the optimal correlation of 0.802 is obtained at $\psi_1 = 37.0$ and $\psi_2 = 38.1$. It seems from the elliptical shapes of the correlation surfaces that the correlation is less sensitive to changes in ψ_2 than in ψ_1, possibly because the background contributes more to the seismic response. But comparing the two wells, it seems that ψ_2 is better determined than ψ_1 since the differences between the two wells in the optimal values of ψ_2 are less. However, it is hard to say from these figures whether ψ_1 and ψ_2 should be different and in that case, whether ψ_1 should be larger that ψ_2 or vice versa.

To summarize, these results show that the seismic response from a heterogeneous sandstone reservoir with thin calcite barriers can be satisfactorily modeled with a convolution model. The correlations between the results from the convolution model and the full waveform reflectivity (f-k) model are about 0.8.

The results also show that both the calcite barriers and the sandstone background contribute to the seismic response. This is clearly seen, even if only the simple convolution model is used. Since the convolution model only includes primary reflections, the results here are in accordance with Bakke (1996) where it is shown that primary reflections account for a relatively large part of the seismic reflections from a thin layer. Furthermore, since the convolution model is linear, it is computationally attractive for use in stochastic modeling schemes where sampling is involved. It has been shown here that the results from use of the convolution models are also acceptable.

References

Abrahamsen, P., Hektoen, A., Holden, L. & Munthe, K. L. (1997), Seismic impedance and porosity: Support effects, *in* E. Baafi & N. Schofield, eds, 'Geostatistics Wollongong

'96', Kluwer Academic Publishers, Dordrecht, 489–500.

Bakke, N. E. (1996), Prediction of Calcite Cement Distribution in Shallow Marine Sandstone Reservoirs using Seismic Data, PhD thesis, Norwegian University of Science and Technology, Department of Petroleum Engineering and Applied Geophysics, NTNU, N-7034 Trondheim, Norway.

Bakke, N. E., Ertresvåg, E. T., Næss, A., MacDonald, A. C. & Fält, L. M. (1996), Application of seismic data and sequence stratigraphy for constraining a stochastic model of calcite cementation, *in* 'SPE European 3-D Reservoir Modelling Conference', Society of Petroleum Engineers, Stavanger, 83–96. SPE 35487.

Behrens, R. A., MacLeod, M. K. & Tran, T. T. (1996), Incorporating seismic attribute maps in 3D reservoir models, *in* 'SPE Annual Technical Conference and Exhibition', Society of Petroleum Engineers, 31–36.

Bjørkum, P. A. & Walderhaug, O. (1990), 'Geometrical arrangement of calcite cementation within shallow marine sandstones', *Earth-Science Reviews* **29**, 145–161.

Bortoli, L.-J., Alabert, F., Haas, A. & Journel, A. (1993), Constraining stochastic images to seismic data: Stochastic simulation of synthetic seismograms, *in* A. Soares, ed.'Geostatistics Tróia '92', Kluwer Academic Publishers, Dordrecht, 325–337.

Doyen, P. M. (1988), 'Porosity from seismic data: A geostatistical approach', *Geophysics* **53**(10), 1263–1275.

Doyen, P. M., Psaila, D. E., den Boer, L. D. & Jans, D. (1997), Reconciling data at seismic and well log scales in 3-D earth modeling, *in* 'SPE Annual Technical Conference and Exhibition', Society of Petroleum Engineers, 465–474.

Eide, A. L. (1999), A stochastic model of porosity and acoustic impedance in a petroleum reservoir, conditioned to seismic data and well data, Preprint, Department of Mathematical Sciences, Norwegian University of Science and Technology, N-7034 Trondheim, Norway.

Eide, A. L., Ursin, B. & Omre, H. (1997), Stochastic simulation of porosity and acoustic impedance conditioned to seismic data and well data, *in* '67th Annual Meeting of the Society of Exploration Geophysicists, Expanded Abstracts', SEG, Dallas, Texas, 1614–1617.

Haas, A. & Dubrule, O. (1994), 'Geostatistical inversion - a sequential method of stochastic reservoir modeling constrained by seismic data', *First Break* **12**(11), 561–569.

Haldorsen, H. H. & Lake, L. W. (1984), 'A new approach to shale management in field scale models', *SPE Journal*, 447–457.

Hastings, W. K. (1970), 'Monte Carlo sampling methods using Markov chains and their applications', *Biometrika* **57**(1), 97–109.

Kennett, B. (1983), *Seismic wave propagation in stratified media*, Cambridge University Press.

Skare, Ø., Skorstad, A., Hauge, R. & Holden, L. (1997), Conditioning a fluvial model on seismic data, *in* E. Baafi & N. Schofield, eds, 'Geostatistics Wollongong '96', Kluwer Academic Publishers, Dordrecht, 465–476.

Stoyan, D., Kendall, W. S. & Mecke, J. (1987), *Stochastic Geometry and its Applications*, John Wiley & Sons, New York.

Syversveen, A. R. & Omre, H. (1997), 'Conditioning of marked point processes within a Bayesian framework', *Scand. J. Statist.* **24**(3), 341–352.

Syversveen, A. R. & Rue, H. (1997), 'A method for approximate fully Bayesian analysis of parameters', *Communications in Statistics; Simulation and Computation* **26**(3), 1147–1162.

Tjølsen, C. B., Johnsen, G., Halvorsen, G., Ryseth, A. & Damsleth, E. (1995), Seismic data can improve the stochastic facies modelling significantly, *in* 'SPE 70th Annual Technical Conference and Exhibition', Society of Petroleum Engineers, 373–379. SPE 30567.

Zhu, H. & Journel, A. G. (1993), Formatting and integrating soft data: Stochastic imaging via the Markov-Bayes algorithm, *in* A. Soares, ed., 'Geostatistics Tróia '92', Kluwer Academic Publishers, Dordrecht, 1–12.

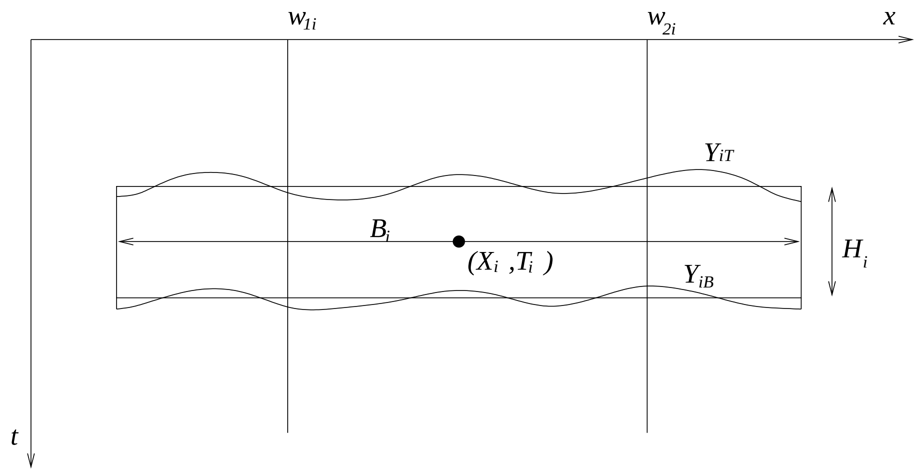

Figure 1: Conceptual model for a single calcite object.

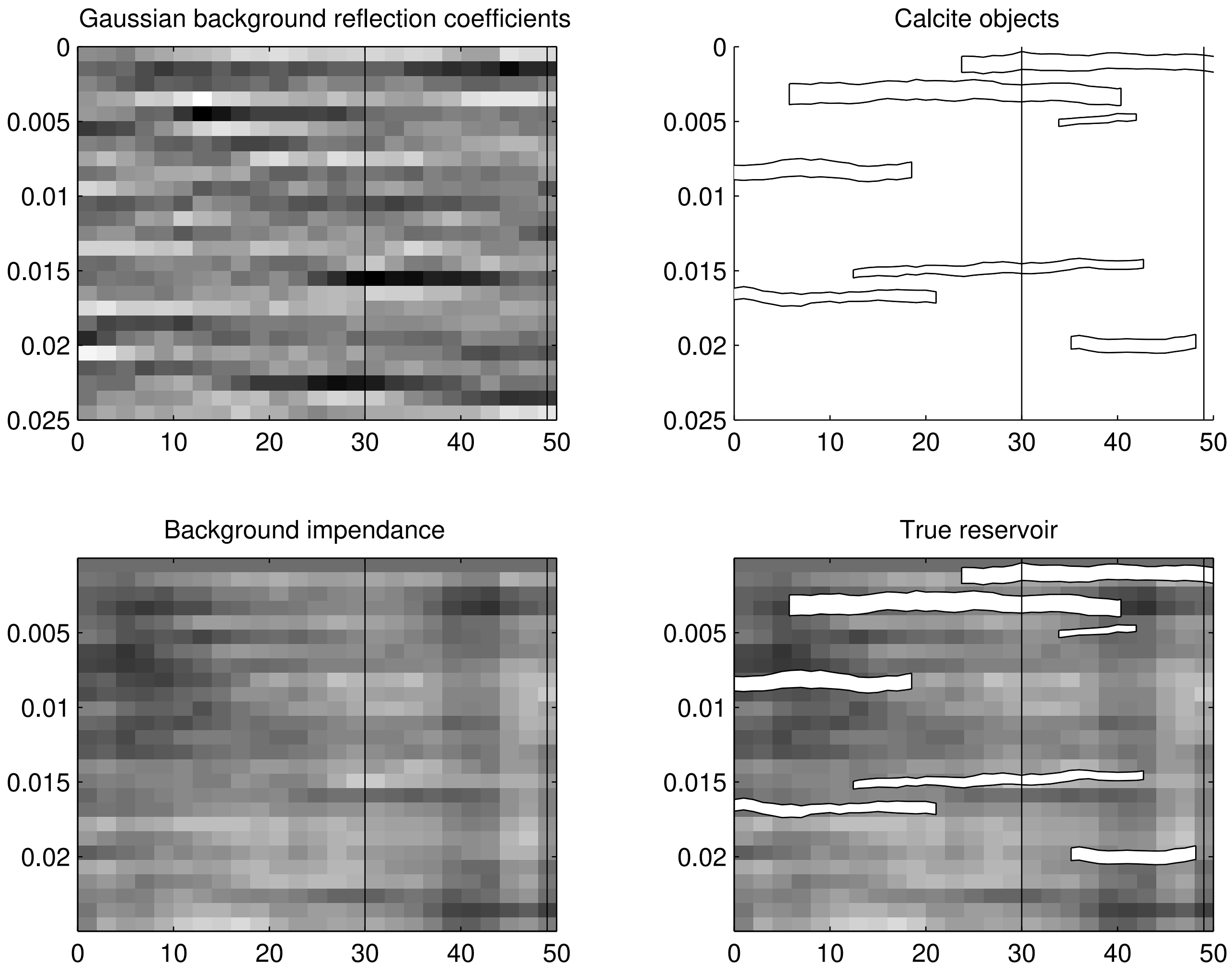

Figure 2: The "true reservoir" generated from the prior model. Upper left: The Gaussian background reflection coefficients. Upper right: The calcites. Lower left: True impedance computed from the reflection coefficients. Lower right: True reservoir: Calcite object superimposed on the background impedance. Vertical lines indicate the position of the two wells.

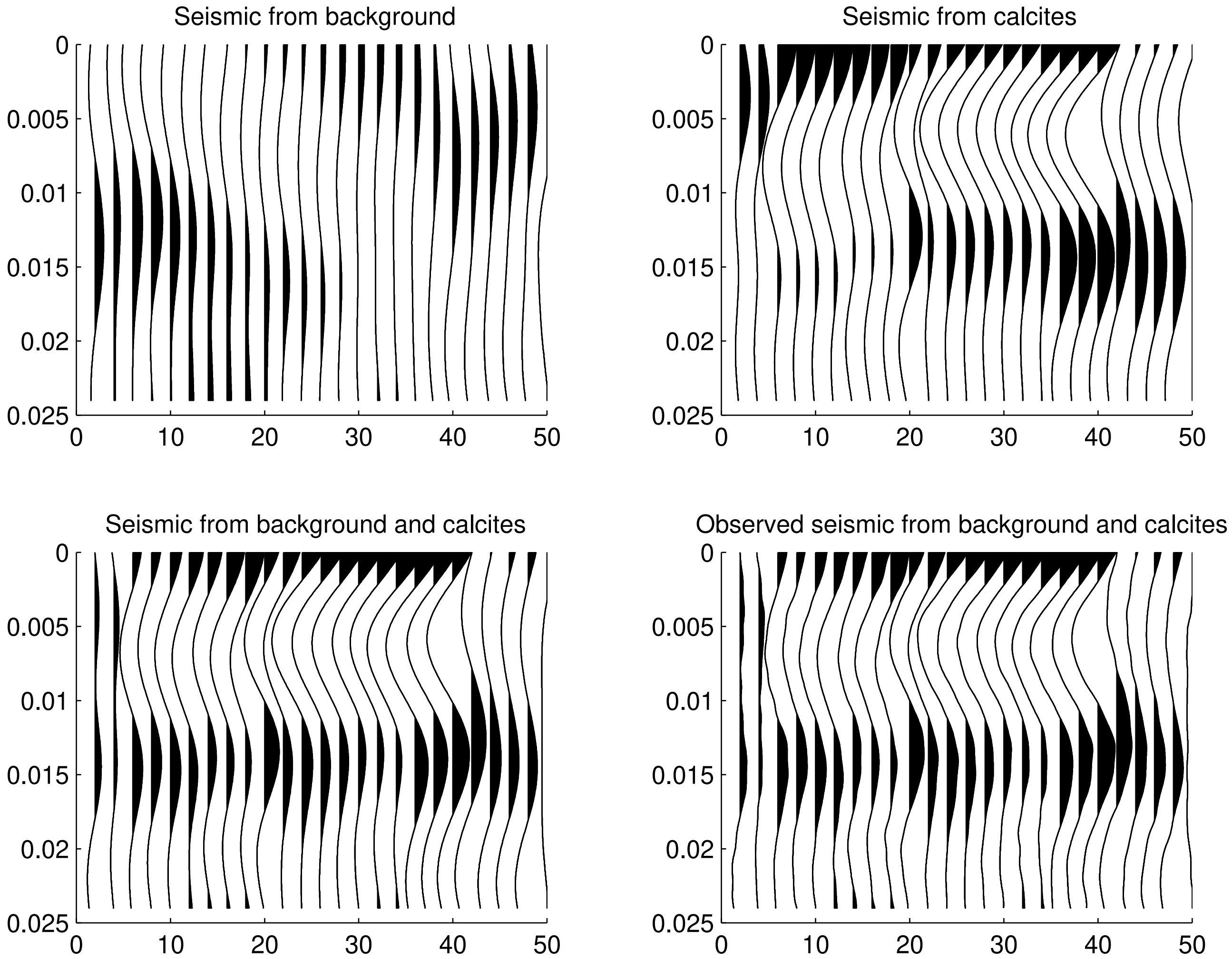

Figure 3: Seismic data from the "true reservoir". Upper left: Seismic response from Gaussian background reflection coefficients. Upper right: Seismic response from calcites. Lower left: Seismic response from background and calcites. Lower right: "Observed" seismic data generated by adding noise to the seismic response from background and calcites.

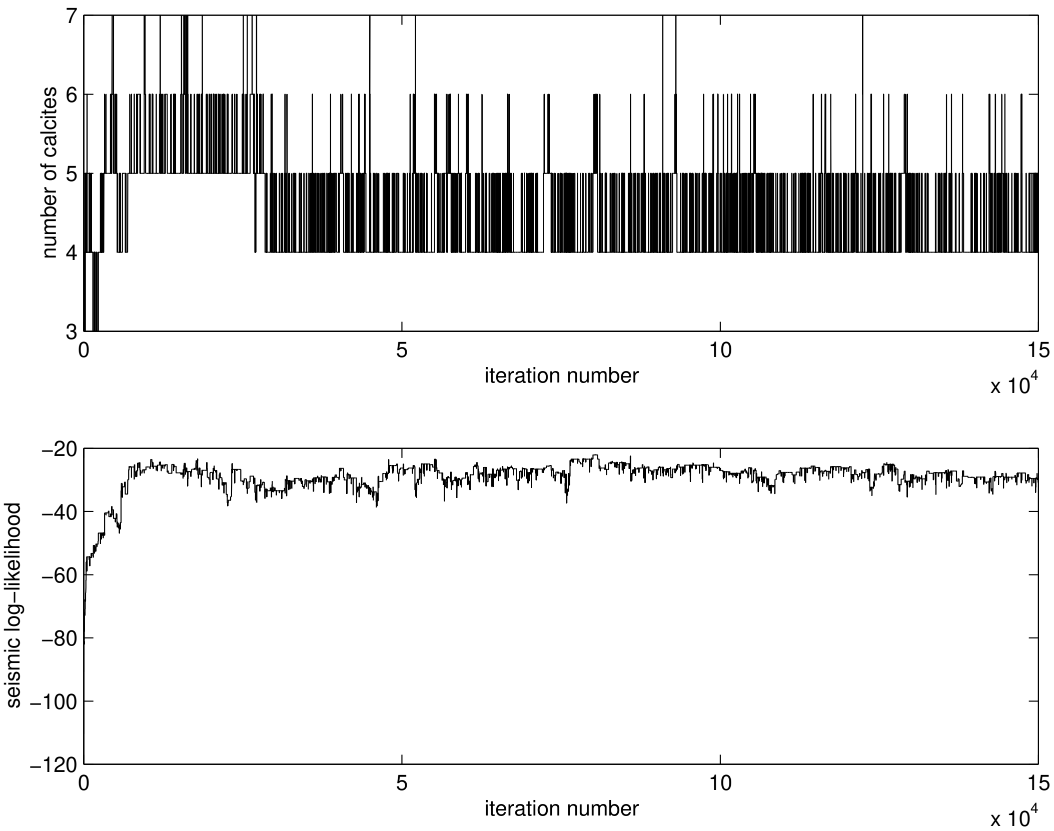

Figure 4: The number of calcites and the seismic log-likelihood function plotted vs the number of iterations in Metropolis-Hastings algorithm.

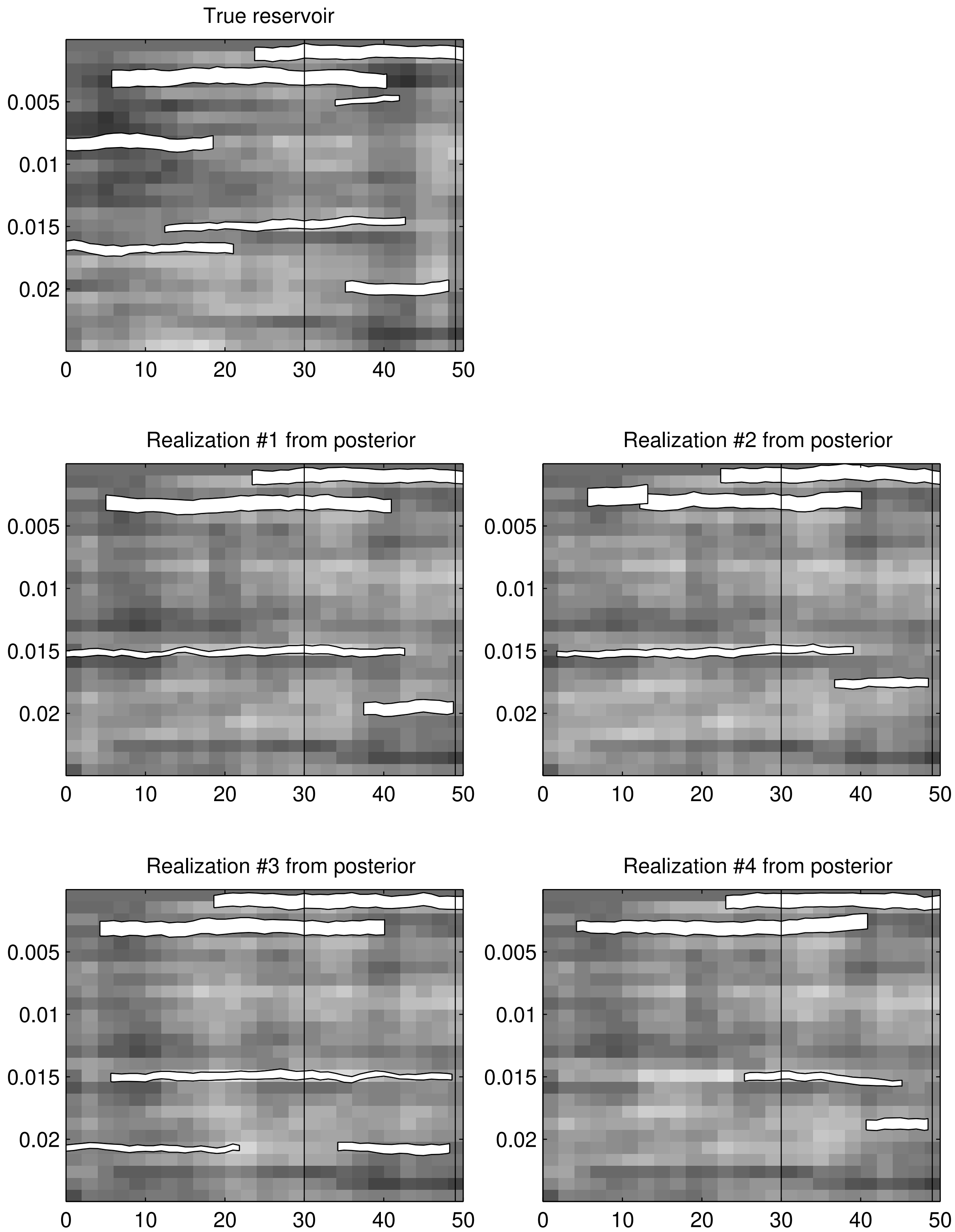

Figure 5: True reservoir and four realizations sampled from the posterior distribution conditioned to seismic data and well data.

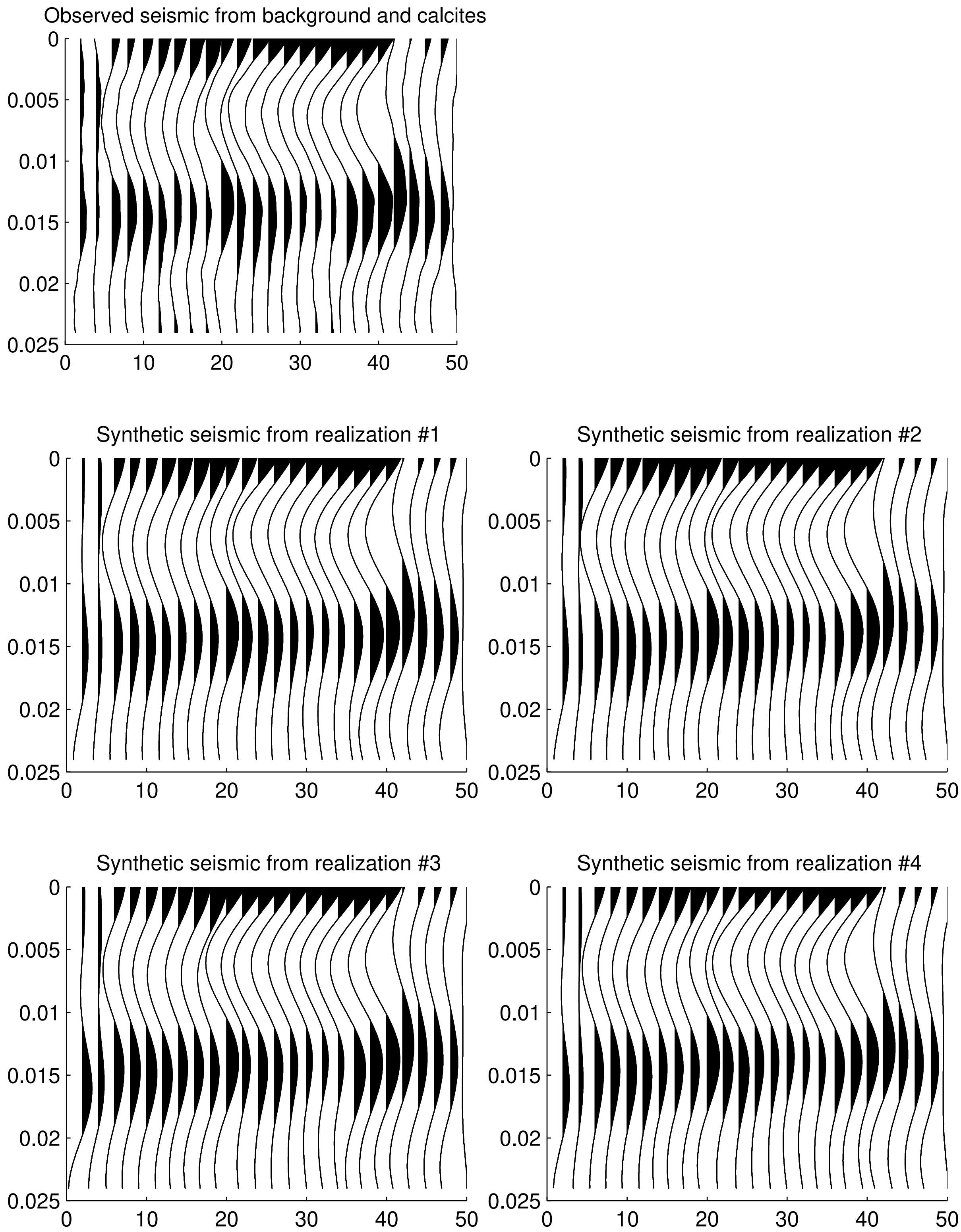

Figure 6: Observed seismic and synthetic seismic corresponding to the four realizations from the posterior distribution.

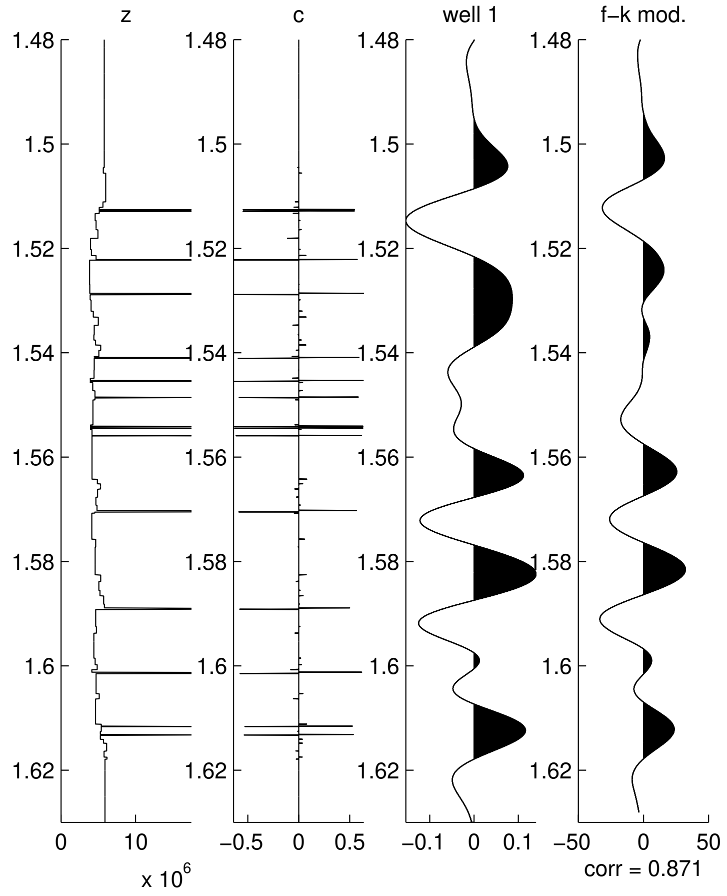

Figure 7: Impedance z, reflection coefficients c and seismic response calculated by convolution for well 1. To the right, the corresponding trace from the full waveform reflectivity (f-k) model is shown. The correlation between the seismic response calculated by convolution and the corresponding trace from the (f-k) model is 0.871.

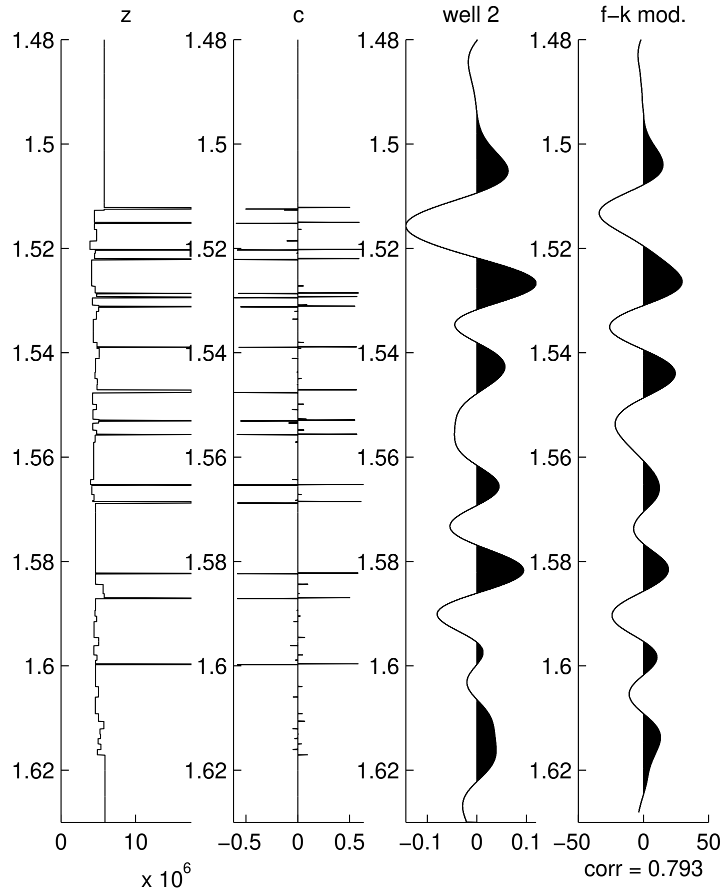

Figure 8: Impedance z, reflection coefficients c and seismic response calculated by convolution for well 2. To the right, the corresponding trace from the full waveform reflectivity (f-k) model is shown. The correlation between the seismic response calculated by convolution and the corresponding trace from the (f-k) model is 0.793.

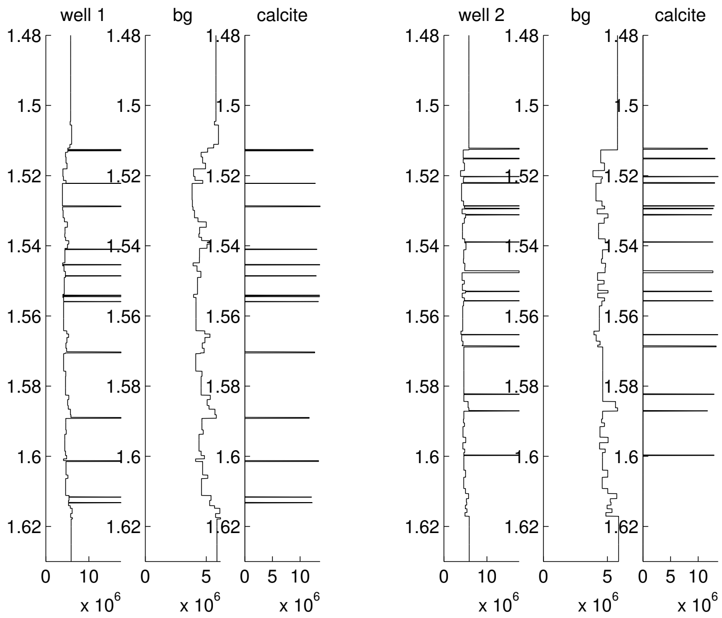

Figure 9: Impedances in well 1 and well 2 split into background and calcite.

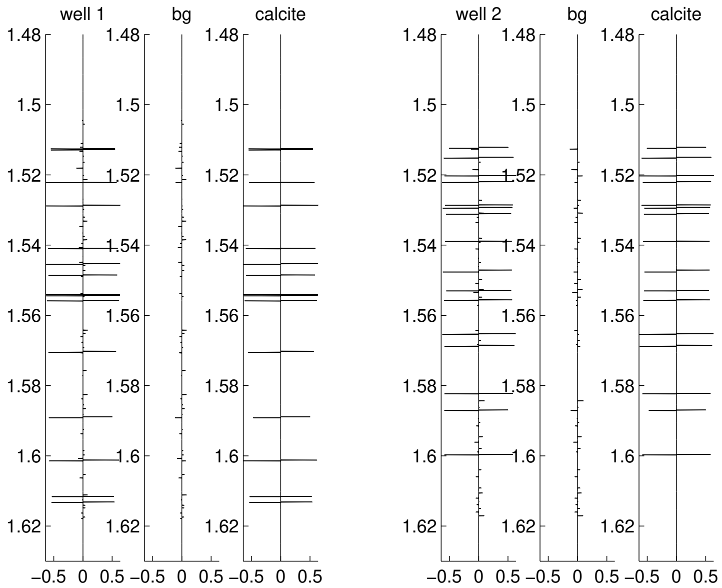

Figure 10: Reflection coefficients in well 1 and well 2 split into background and calcite.

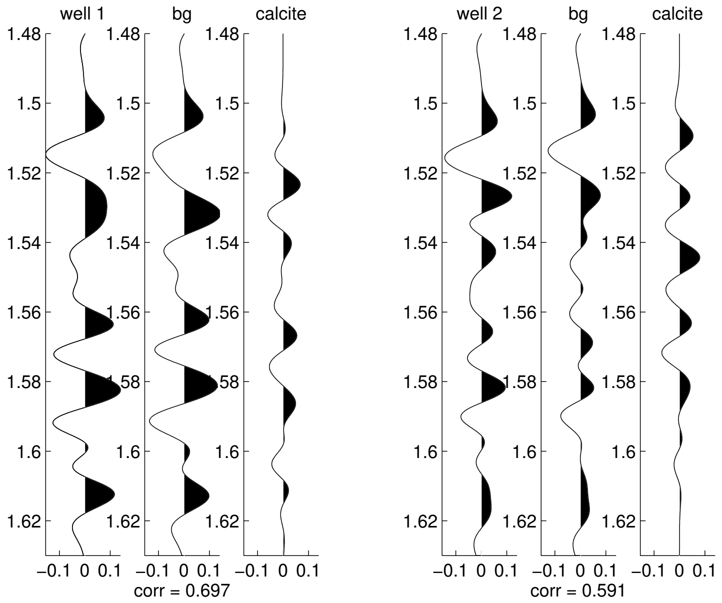

Figure 11: Seismic response from background and calcite, calculated by convolution of a 40 Hz Ricker wavelet with the reflection coefficients shown in Figure 10.

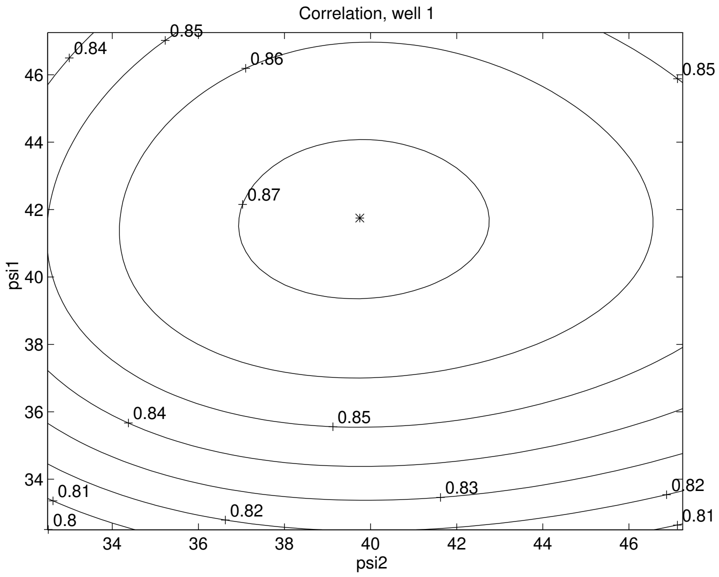

Figure 12: Correlations between seismic response calculated with convolution model and full waveform model for well 1.

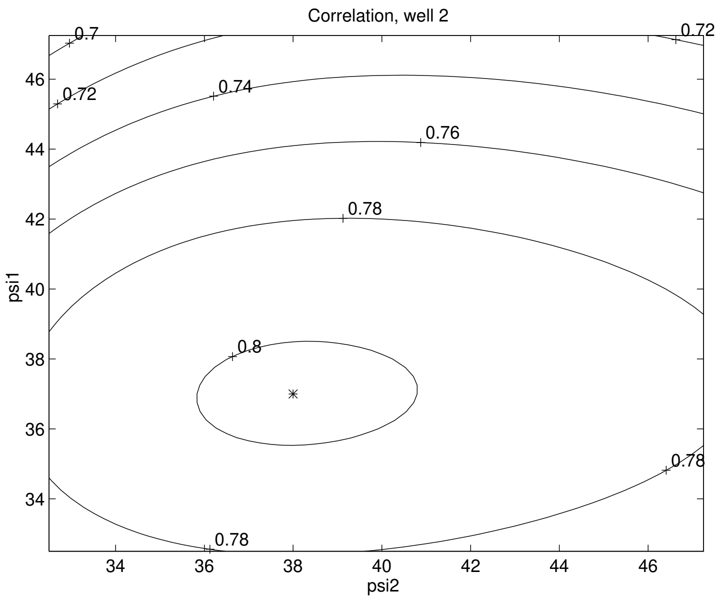

Figure 13: Correlations between seismic response calculated with convolution model and full waveform model for well 2.